DOI: 10.1002/ejic.201100898

Synthesis, Characterisation, and Preliminary In Vitro Studies of Vanadium(IV) Complexes with a Schiff Base and Thiosemicarbazones as Mixed Ligands

Nerissa A. Lewis,[a] Fange Liu,[b] Luke Seymour,[a] Anthony Magnusen,[a] Travis R. Erves,[a] Jessa Faye Arca,[a] Floyd A. Beckford,[c] Ramaiyer Venkatraman,[d] Antonio González-Sarrías,[e] Frank R. Fronczek,[f] Don G. VanDerveer,[g] Navindra P. Seeram,[e] Aimin Liu,[b] William L. Jarrett,[h] and Alvin A. Holder*[a]

Keywords: Bioinorganic chemistry / Medicinal chemistry / Antitumor agents / Vanadium / ^{51}V NMR / EPR spectroscopy

[VO(sal-L-tryp)(H_2O)] (**1**, sal-L-tryp = *N*-salicylidene-L-tryptophanate) was used as a precursor to produce the new complexes [VO(sal-L-tryp)(MeATSC)]·1.5C_2H_5OH [**2**, MeATSC = 9-Anthraldehyde-*N*(4)-methylthiosemicarbazone], [VO(sal-L-tryp)(*N*-ethhymethohcarbthio)]·H_2O [**3**, *N*-ethhymethohcarbthio = (*E*)-*N*-ethyl-2-(4-hydroxy-3-methoxybenzylidene)-hydrazinecarbothioamide] and [VO(sal-L-tryp)(acetylethTSC)]·C_2H_5OH {**4**, acetylethTSC = (*E*)-*N*-ethyl-2-[1-(thiazol-2-yl)ethylidene]hydrazinecarbothioamide} by reaction with the respective thiosemicarbazone. The chemical and structural properties of these ligands and complexes were characterised by elemental analysis, ESI-MS, FTIR, UV/Vis, ESR and ^{1}H and ^{13}C NMR spectroscopy and X-ray crystallography. Dimethyl sulfoxide (DMSO) and [D_6]DMSO solutions of **1**–**4** were oxidised in air to produce vanadium(V) species, which were verified by ESI-MS and ^{51}V NMR spectroscopy. The anticancer properties of **2**–**4** were examined with three colon cancer cell lines, HTC-116, Caco-2 and HT-29, and noncancerous colonic myofibroblasts, CCD18-Co. Compounds **2**–**3** exhibited less inhibitory effects in the CCD-18Co cells, which indicates a possible cytotoxic selectivity towards colon cancer cells. In general, compounds that exhibit antiproliferative activity to cancer cells but do not affect noncancerous cells may have a potential in chemotherapy.

Introduction

The limited efficacy of current treatments for advanced colon cancer serves an impetus for a concerted effort to identify chemopreventive agents for treatment. This process has always involved metal complexes. Cisplatin is widely used for the treatment of many cancers[1] despite its high toxicity, undesirable side effects and problems with drug resistance in primary and metastatic cancers.[2] These limitations have spurred a growing interest in new nonplatinum metal complexes that show anticancer properties.[3] Ruthenium has been reported to possess several favourable properties suited to rational anticancer drug design,[4] and ruthenium complexes of various types are being studied as metallodrugs as they are believed to have low toxicity and good selectivity for tumors.[5] Recently, we reported the effect of ruthenium(II) complexes with new chelating thiosemicarbazones on the growth inhibition of MCF-7 and MDA-MB-231 (breast adenocarcinoma) and HCT 116 and HT-29 (colorectal carcinoma) cell lines.[6] Thiosemicarbazones and their metal complexes are used in many applications ranging from pharmacology to nuclear medicine.[7]

Here we present our efforts to expand our study of non-ruthenium systems. There have been few systematic studies of the use of vanadium compounds as potential anticancer agents, for example, there has been a report of vanadium(V) complexes with salicylaldehyde semicarbazone derivatives that featured in vitro antitumour activity towards kidney tumour cells (TK-10).[8] In addition, several vanadium(IV) compounds are known to exhibit anticancer activities.[9] Previously, bis(4,7-dimethyl-1,10-phenanthroline)sulfato-

[a] Department of Chemistry and Biochemistry, The University of Southern Mississippi,
118 College Drive, # 5043, Hattiesburg, MS 39406-0001, U.S.A.
Fax: +1-601-266-6075
E-mail: alvin.holder@usm.edu
[b] Department of Chemistry, Georgia State University,
P. O. Box 4098, Atlanta, GA 30302, U.S.A.
[c] Science Division, Lyon College,
Batesville, AR 72501, U.S.A.
[d] Department of Chemistry and Biochemistry, Jackson State University,
P. O. Box 17910, 1400 JR Lynch Street, Jackson, MS 39217, U.S.A.
[e] Bioactive Botanical Research Laboratory, Department of Biomedical and Pharmaceutical Sciences, College of Pharmacy, University of Rhode Island,
Kingston, RI 02881, U.S.A.
[f] Department of Chemistry, Louisiana State University,
Baton Rouge, LA 70803, U.S.A.
[g] Molecular Structure Centre, Chemistry Department, Clemson University
Clemson, SC 29634-0973, U.S.A.
[h] School of Polymers and High-Performance Materials, The University of Southern Mississippi,
118 College Dive, #5050, Hattiesburg, MS 39406-0076, U.S.A.
Supporting information for this article is available on the WWW under http://dx.doi.org/10.1002/ejic.201100898.

oxovanadium(IV) (metvan) was identified as the most promising multitargeted anticancer compound with apoptosis-inducing activity.[9c]

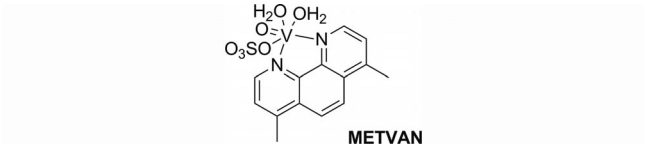

Interestingly, metvan was found to be highly effective against cisplatin-resistant ovarian and testicular cancer cell lines.[9c] Given the paucity of data regarding the use of vanadium(IV) complexes with thiosemicarbazones as ligands as potential anticancer agents, we now report the synthesis and chemical characterisation of a series of such complexes and the preliminary results of a biological study against several colorectal cancer cell lines in order to evaluate their potential as chemotherapeutic candidates.

Results and Discussion

All compounds were characterised by elemental analysis. The structural components of the ligands and complexes were confirmed by FTIR, ^{1}H and ^{13}C NMR spectroscopy, MS and X-ray crystallography, where appropriate.

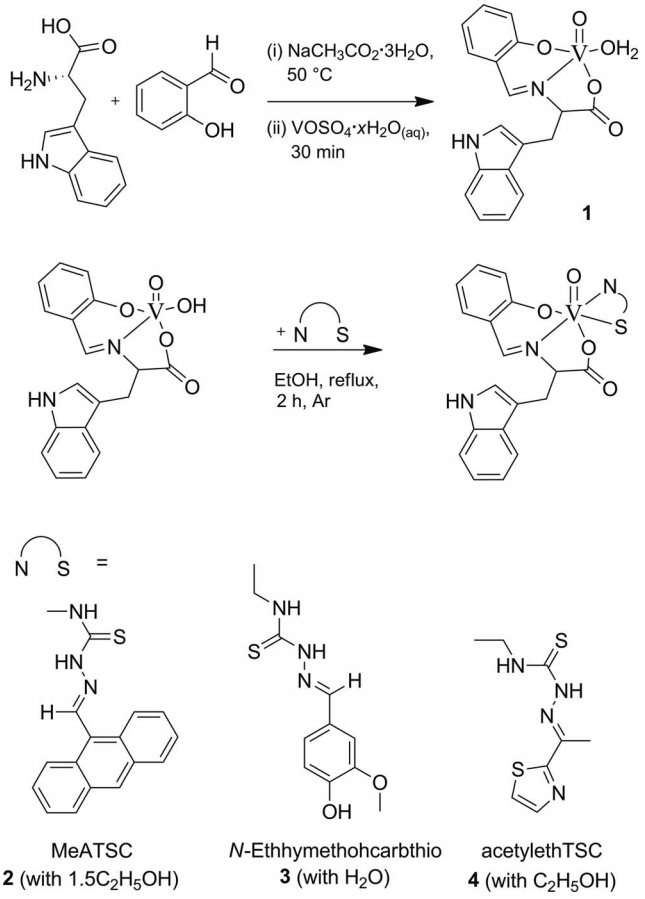

Scheme 1. Synthesis of **1**–**4**.

Chemistry and Pharmacology

9-Anthraldehyde-*N*(4)-methylthiosemicarbazone (MeATSC) was synthesised as described by Beckford et al.[6] and two new thiosemithiocarbazones, (*E*)-*N*-ethyl-2-(4-hydroxy-3-methoxybenzylidene)hydrazinecarbothioamide (*N*-ethhymethohcarbthio) and (*E*)-*N*-ethyl-2-[1-(thiazol-2-yl)-ethylidene]hydrazinecarbothioamide (acetylethTSC), were also synthesised (Scheme S1, Supporting Information). 2-(2-Hydroxybenzylamino)-3-(1*H*-indol-3-yl)propanoic acid (the reduced Schiff base) was prepared using a known procedure,[10] which involved salicylaldehyde, amino acids and $NaBH_4$ with L-tryptophan (Scheme S2). [VO(sal-L-tryp)-(H_2O)] (**1**, sal-L-tryp = *N*-salicylidene-L-tryptophanate) was prepared as described by Pessoa et al.[11] [VO(sal-L-tryp)-(MeATSC)]·1.5C_2H_5OH (**2**), [VO(sal-L-tryp)(*N*-ethhymethohcarbthio)]·H_2O (**3**) and [VO(sal-L-tryp)(acetylethTSC)]·C_2H_5OH (**4**) were synthesised by the reaction of **1** with the respective thiosemicarbazones (Scheme 1). Compounds **2**–**4** were isolated in yields of 57–78%.

In this study, we investigated the cytotoxic effects of our complexes against three colon cancer cell lines, HTC-116, Caco-2 and HT-29, along with a comparative antiproliferative study of noncancerous colonic myofibroblasts, CCD-18Co, by using the standard 3-(4,5-dimethylthiazol-2-yl)-5-(3-carboxymethoxyphenyl)-2-(4-sulfenyl)-2*H*-tetrazolium, inner salt (MTS)-dye reduction assay for cell viability.

Elemental Analyses and MS

Elemental analysis was carried out on *N*-ethhymethohcarbthio and **1**–**4**. The percentage of N found in **4** was 10.91% vs. the calculated value of 12.98%. The elemental analysis data for the percentage of N is not fully consistent with the calculated value, but other spectroscopic methods confirmed the identity of **4**. Due to the fact that the discrepancy is only in the nitrogen, it is likely due to an error in the analysis process or the loss of ethanol as solvate during the analytical procedure. However, ESI-MS proved the existence of [VO(sal-L-tryp)(acetylethTSC)] without ethanol as a solvate.

ESI mass spectra were acquired for **2**–**4** and the products obtained from oxidised DMSO solutions of **1** and **3** (Figures S1–S9 and Schemes S3–S5). The results thus obtained are in agreement with a metal/ligand ratio of 1:1 in the complexes. Table 1 shows the ESI-MS data acquired for the ligands and complexes (Figures S1–S9). Overall, the suggested formulae were further confirmed by mass spectral fragmentation analysis.

Oxidovanadium(IV) complexes that contain *N*-salicylidene-L-amino acid ligands can be oxidised to form vanadium(V) compounds.[12] It was important to determine whether our vanadium(IV) complexes could be oxidised to form vanadium(V) species when dissolved in DMSO. Com-

Table 1. MS data for ligands and complexes.

A) Reduced Schiff base, K[sal-L-tryp] and **1**–**4**

Species	Exact mass [g mol^{-1}]	Species formed in the spectrometer	*m*/*z*	Relative int. [%]
Reduced Schiff base[a]	310.13	$[M + H]^+$	311.08	100.00
		$[M – CHO_3 + H]^+$	242.42	13.04
		$[2M + H]^+$	620.36	12.77
		$[3M + H]^+$	930.39	5.02
		$[4M + H]^+$	1240.92	3.92
K[(sal-L-tryp)][a]	346.07	$[M + H]^+$	344.05	39.65
		$[M – OH – K + H]^+$	300.03	100.00
		$[M – OH – O – K + H]^+$	205.20	50.43
		$[M – COO – K + H]^+$	242.62	64.65
		$[M – COO – OH – K + H]^+$	262.12	1.51
		$[M – C_7H_6O – K + H]^+$	281.14	46.08
[VO(sal-L-tryp)(MeATSC)][a]	666.14	$[M + H]^+$	666.17	100.00
		$[M – C_2H_5N_2S + H]^+$	577.08	33.10
		$[M – C_{17}H_{17}N_3 + H]^+$	405.14	31.86
		$[MeATSC + H]^+$	292.14	54.60
[VO(sal-L-tryp)(*N*-ethhymethohcarbthio)][b]	626.13	$[M – H]^–$	624.87	100.00
		$[M – C_{11}H_{10}N_2O – H]^–$	431.90	64.75
		$[M – C_{11}H_{15}N_3O_2S – H]^–$	407.85	20.99
		$[[C_{11}H_{15}N_3O_2S – C_8H_7N] – H]^–$	287.88	12.70
		$[N$-ethhymethohcarbthio $– H]^–$	252.00	25.74
[VO(sal-L-tryp)(acetylethTSC)][a]	601.09	$[M + H]^+$	600.25	2.71
		$[M – C_3H_7NS + H]^+$	513.57	100.00
		$[M – C_7H_5NO + H]^+$	482.38	37.11
		$[M – C_{17}H_{15}N_2O + H]^+$	336.06	4.13

B) Oxidised products isolated from **1** and **3**.

Species	Exact mass [g mol^{-1}]	Species formed in the spectrometer	*m*/*z*	Relative int. [%]
Proposed [VO(sal-L-tryp)(DMSO)(OH)][c,a] intermediate	468.06	$[M + H]^+$	468.60	1.67
		$[M – OH – DMSO – C_8H_7N + H]^+$	242.41	100.00
		$[M – OH + H]^+$	451.05	48.25
		$[[V_2O_3(sal\text{-}L\text{-}tryp)_2] + H]^+$	763.68	30.06
		$[[V_2O_3(sal\text{-}L\text{-}tryp)_2(H_2O)] + H]^+$	776.77	49.36
		$[[V_2O_3(sal\text{-}L\text{-}tryp)_2(DMSO)_2] + H]^+$	918.28	3.13
Proposed [VO(sal-L-tryp)(DMSO)(OH)][d,a] intermediate	468.06	$[M + H]^+$	470.01	0.50
		$[N$-ethhymethohcarbthio $+ H]^+$	252.26	100.00
		$[M – OH + H]^+$	451.96	2.97
		$[M – OH + N$-ethhymethohcarbthio $+ H]^+$	702.75	2.15
		$[[V_2O_3(sal\text{-}L\text{-}tryp)_2] + H]^+$	763.22	0.74
		$[[V_2O_3(sal\text{-}L\text{-}tryp)_2(H_2O)] + H]^+$	775.40	1.08
		$[[V_2O_3(sal\text{-}L\text{-}tryp)_2(DMSO)_2] + H]^+$	916.44	0.75

[a] Positive mode. [b] Negative mode. [c] Proposed vanadium(V) intermediate obtained from **1**. [d] Proposed vanadium(V) intermediate obtained from **3**.

pounds **1** and **3** were dissolved in DMSO, and the resulting solutions were allowed to evaporate to leave a solid. ESI-MS was carried out on the remaining solids and showed that **1** and **3** were oxidised to form vanadium(V) species (Table 1). Vanadium(V) species with coordinated DMSO were detected by ESI-MS. Scheme 2 shows a proposed mechanism for the formation of the oxidised compounds in DMSO.

X-ray Crystallographic Studies on acetylethTSC

A single crystal of acetylethTSC was grown by the slow evaporation of a methanol solution. The molecular structure of acetylethTSC together with the atomic numbering scheme is shown in Figure 1, and Table 2 shows the crystal data and structure refinement for acetylethTSC.

Thiosemicarbazones are known to exhibit thione–thiol tautomerism.[6] The crystal structure shows that acetylethTSC exists as a thione in the solid state. The C(1)–S(1) distance (1.6814 Å) is similar to that found in a methyl analogue of 2-acetyl-2-thiazoline thiosemicarbazone, which is in the thione form as a solid.[13] AcetylethTSC adopts a *syn* conformation about the N1–N2 bond in a similar fashion as thiosemicarbazones formed from 2-acetylthiazole.[14] The N2–H group donates an intermolecular hydrogen bond to thione S1 to form centrosymmetric hydrogen-bonded dimers with an N···S distance of 3.4651(15) Å. The thiazole N4 atom is not involved in hydrogen bonding as shown in Figure 2.

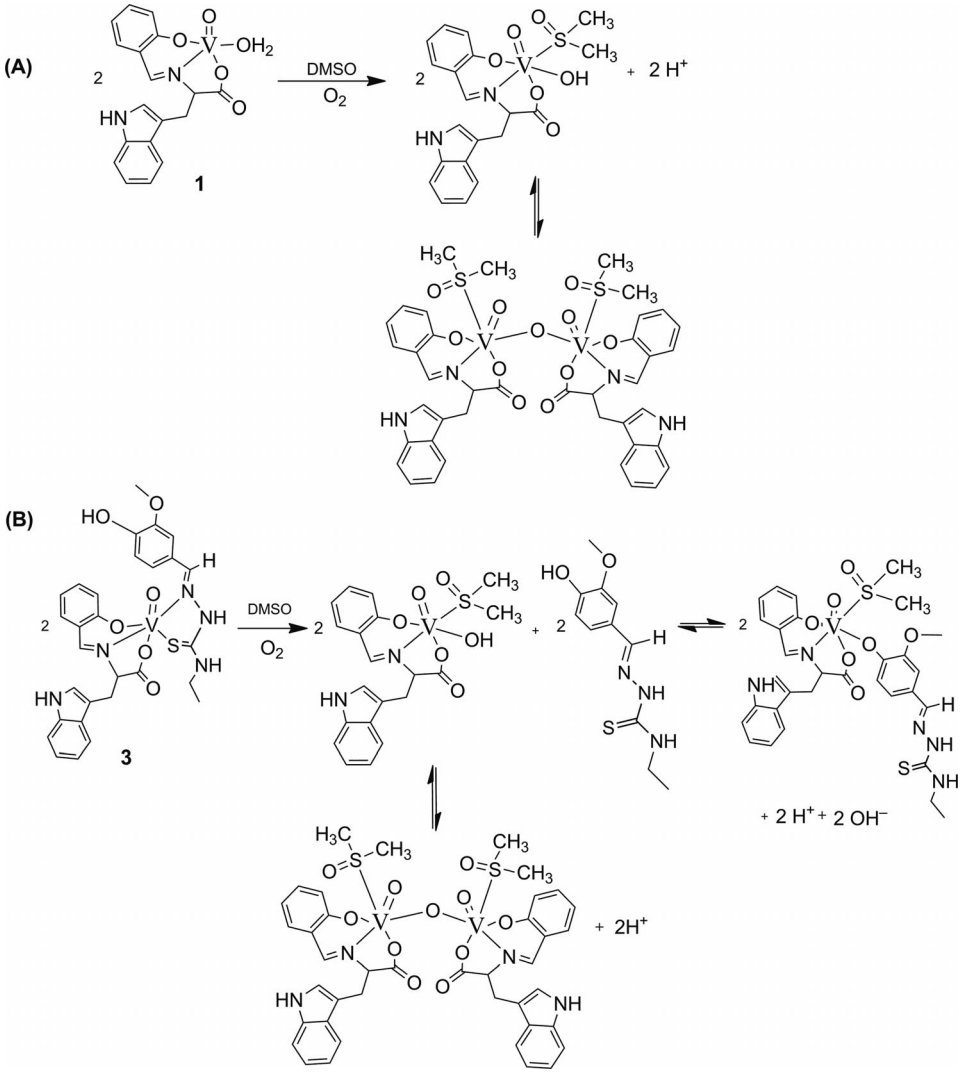

Scheme 2. Proposed mechanism for the formation of the oxidised compounds in DMSO.

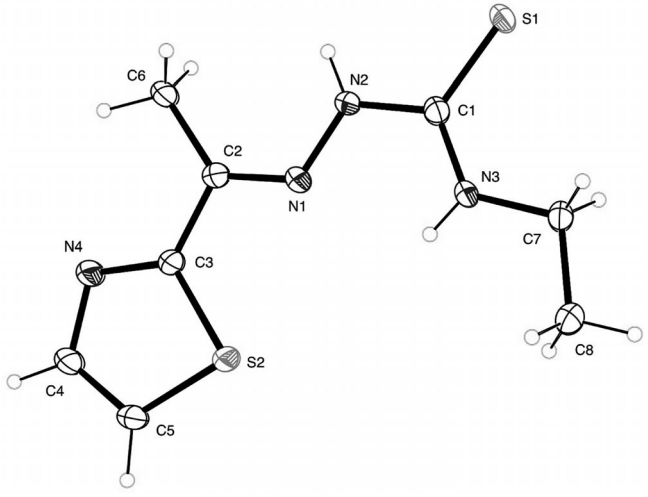

Figure 1. A thermal ellipsoid plot (50% probability envelopes) of acetylethTSC.

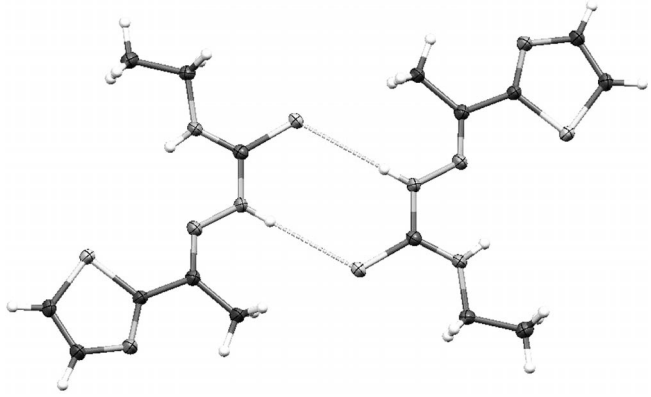

Figure 2. Hydrogen bonding in acetylethTSC.

FTIR Spectroscopy

Infrared spectra were acquired for the ligands and complexes (Figures S10–S18). Thiosemicarbazones exhibit char-

Table 2. Crystal data and structure refinement for acetylethTSC.

	acetylethTSC
Empirical formula	$C_8H_{12}N_4S_2$
Formula weight	228.34
Temperature	90.0(5) K
Wavelength	1.54178 Å
Crystal system, space group	monoclinic, *C*2/*c*
Unit cell dimensions	a = 10.4549(10) Å, α = 90° b = 10.8970(10) Å, β = 91.544(5)° c = 18.7694(15) Å, γ = 90° V = 2137.6(3) Å^3
Z, calculated density	8, 1.419 Mg/m^3
Absorption coefficient	4.251 mm^{-1}
F(000)	960
Crystal size	0.18 × 0.17 × 0.09 mm
Theta range for data collection	5.8 to 68.1°
Limiting indices	$-12 \le h \le 12$, $-12 \le k \le 13$, $-22 \le l \le 22$
Reflections collected/unique	8017/1901 [R_{int} = 0.026]
Completeness to θ = 66.6°	99.1%
Absorption correction	Semi-empirical from equivalents
Max. and min. transmission	0.701 and 0.515
Refinement method	Full-matrix least squares on F^2
Data/restraints/parameters	1901/0/136
Goodness-of-fit on F^2	1.065
Final R indices [$I > 2\sigma(I)$]	R_1 = 0.0276, wR_2 = 0.0691
R indices (all data)	R_1 = 0.0312, wR_2 = 0.0715
Extinction coefficient	0.00011(3)
Largest diff. peak and hole	0.257 and –0.262 e Å^{-3}

acteristic bands that correspond to various functional groups in different energy regions. The most significant bands in the 4000–500 cm^{-1} region are found between 3100–3500 (NH stretching vibrations), 1580–1630 (C=N and NH), and 1100–1300 and 820–900 (C=S). Thiosemicarbazones can coordinate as either a neutral (thione) or a monoanionic (thiolate) ligand.[15] The ligands (Figures S10–S12) here all seem to be in the thione form in the solid state.[16] This was inferred primarily from the absence of a ν(S–H) absorption in the 2600–2500 cm^{-1} region. There are two bands in the ν(N–H) region, and the presence of the peak due to the hydrazinic hydrogen atom confirms the thione formulation. The thiolate form was not evident in our compounds in the solid state (see Tables 3 and 4 for the respective stretching frequencies for the ligands and complexes).

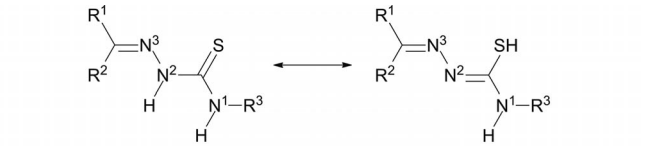

Tautomerism in thiosemicarbazones

IR spectra of all the complexes (Figures S15–S18) show a band in the ν(N–H) region that may be attributed to the hydrazinic nitrogen atom and suggests that the ligands are coordinated as the thione form. Neither the hydrazinic nor the terminal (aminic) hydrogen atom shifted significantly upon coordination of the ligand. The ligands all show a medium intensity band in the 1620–1605 cm^{-1} region, which is assigned as the C=N (imine) linkage. On coordination of the ligand, this band shifts significantly for acetylethTSC (1607–1621 cm^{-1} in **4**) and *N*-ethhymethohcarbthio (1605 to 1616 cm^{-1} in **3**). The stretching frequency of MeATSC changed slightly on coordination to **1**. The shift in this band is indicative of the involvement of the iminic nitrogen atom in the ligation.[7b,17] The involvement of the thiocarbonyl group in the binding can be similarly inferred from the fact that the peaks changed frequency to lower wavenumbers on coordination to **1** (6 cm^{-1} for **2**, 11 cm^{-1} for **3** and 2 cm^{-1} for **4**). The magnitude of the shifts suggest that the ligands coordinate in their neutral bidentate form (through the iminic nitrogen and the thiocarbonyl sulfur atoms) in all the complexes.

A ν(V–S) stretching frequency is observed in the 470–400 cm^{-1} region for all complexes. The absence of a similar band in the spectra of the free thiosemicarbazone ligands confirms coordination by the thiocarbonyl sulfur atom. IR spectra of the reduced Schiff base and K[sal-L-tryp] (Figures S13 and S14) were used to assign the important stretching frequencies due to the coordination of the Schiff base moiety. A phenolate ν(C–O) stretching frequency in the 1545–1540 cm^{-1} region is observed for **1**–**4**. Broad ν(OH) stretching frequencies are observed at 3014 and 3010 cm^{-1} for **1** and **3**, respectively. The absence of the ν(O–H) stretching frequencies of the phenol in **2** and **4** confirms the coordination of the ligand to the vanadium(IV) centre by the phenolate anion.[18]

Table 3. FTIR spectroscopic data [cm^{-1}] for the ligands.

	Indolic ν(NH)	–N^{1}H$_2$ ν(NH)	N^{2}H ν(NH)	ν(N–N)	ν(C–O)	ν_s(COO)	ν_{as}(COO)	TSC ν(C=N)	sal-L-tryp ν(C=N)	ν(C=S)	ν(V–S)	ν(OH)
MeATSC	–	3399 (m)	3201 (w)	1075 (m)	–	–	–	1621 (m)	–	1255 (m), 841 (m)	–	–
N-Ethhyme-thohcarbthio	–	3304 (m)	3300 (w)	1155 (m)	–	–	–	1606 (m)	–	1267 (m), 831 (m)	–	3130 (br.)
AcetylethTSC	–	3164 (m)	3054 (w)	1059 (m)	–	–	–	1543 (m)	–	1296 (m), 813 (m)	–	–
K[(sal-L-tryp)]	3407 (m)	–	–	–	1194 (m)	1521 (m)	1604 (m)	–	1570 (m)	–	–	3169 (br.)
Reduced Schiff base ligand	3392 (m)	–	–	–	1208 (m)	1494 (m)	1592 (m)	–	–	–	–	3055 (br.)

Table 4. FTIR spectroscopic data [cm^{-1}] for the complexes.

A) Compounds **1**–**4**

	Indolic ν(NH)	$-N^1H_2$ ν(NH)	N^2H ν(NH)	ν(N–N)	ν(C–O)	ν_s(COO)	ν_{as}(COO)	TSC ν(C=N)	sal-L-tryp ν(C=N)	ν(C=S)	ν(V–S)	ν(V=O)	ν(OH)
1	3478 (m)	–	–	–	1540 (m)	1490 (m)	1597 (s)	–	1600 (m)	–	–	997 (s)	3014 (br.)
2	3200 (m)	3340 (m)	2976 (w)	1148 (m)	1544 (m)	1491 (m)	1600 (s)	1624 (m)	1590 (m)	1225 (m), 829 (m)	455 (m)	980 (s)	–
3	3210 (m)	3306 (m)	2970 (w)	1154 (m)	1540 (m)	1480 (m)	1600 (s)	1620 (m)	1580 (m)	1270 (m), 802 (m)	454 (m)	976 (s)	3010 (br.)
4	3229 (m)	3310 (m)	2976 (w)	1149 (m)	1545 (m)	1480 (m)	1600 (s)	1624 (m)	1580 (m)	1287 (m), 819 (m)	455 (m)	982 (s)	–

B) Oxidised products isolated from compounds **1** and **3**

	Indolic ν(NH)	ν(C–O)	ν_s(COO)	ν_{as}(COO)	TSC ν(C=N)	sal-L-tryp ν(C=N)	ν(V=O)	ν(OH)	ν(S=O)
A – oxidised product obtained from **1**	3185 (m)	1551 (m)	1497 (m)	1618 (s)	–	1581 (m)	949 (s)	3194 (br.)	1164 (m), 1213 (m)
B – oxidised product obtained from **3**	3201 (m)	1550 (m)	1497 (m)	1600 (s)	1666 (m)	1590 (m)	946 (s)	3193 (br.)	1133 (m), 1157 (m)

All complexes exhibited ν(V=O) stretching frequencies in the 997–980 cm^{-1} region, which is the typical range for oxidovanadium(IV) complexes.[19] Upon coordination of the respective thiosemicarbazone ligands to **1**, a decrease of the V=O stretching frequency occurred, i.e. a change of 17 cm^{-1} in **2**, 21 cm^{-1} in **3** and 15 cm^{-1} in **4**.

NMR Spectroscopy

^{1}H and ^{13}C NMR Spectroscopy

^{1}H and ^{13}C NMR spectra were acquired for *N*-ethhymethohcarbthio, acetylethTSC, the reduced Schiff base, K[sal-L-tryp] and the oxidised products derived from **1** and **3** (Figures S19–S26). Figure 3 shows the ^{1}H NMR spectra of *N*-ethhymethohcarbthio and acetylethTSC.

N-Ethhymethohcarbthio and AcetylethTSC

The presence of singlets at δ = 11.42 and 10.59 ppm in the ^{1}H NMR spectra of *N*-ethhymethohcarbthio and acetylethTSC, respectively, are labelled as g in part A and as e in part B of Figure 3.[20] It is common for this signal to be used as a diagnostic test for the identification of *E* and Z isomers.[6] According to Afrasiabi,[21] a chemical shift at δ = 13–15 ppm proves that the ligand is in the *E* form, whereas a peak at δ = 9–12 ppm proves that the ligand is in the *Z* form. Based on this analysis and coupled with the lack of a signal at $\delta \approx 4.0$ ppm, which is attributed to a SH proton resonance, it can be inferred that both ligands exist as the *Z* isomer. An X-ray crystallographic study on acetylethTSC confirmed the existence of the thione moiety in the free ligand. We also believe that the chemical shift of 13.2 ppm for acetylethTSC (Figure 3, B) is due to equilibrium in solution between the hydrogen-bonded (Z-conformation) and the non-hydrogen-bonded (*E*-conformation) forms.

Oxidised Products Isolated from 1 and 3

It is important to determine the species that are formed when **1** and **3** are oxidised in DMSO. In order to determine such species, ^{1}H NMR spectra were acquired of the isolated oxidised products. All ^{1}H NMR spectra exhibited broad signals (Figures S21 and S22). This is attributed to the presence of some residual paramagnetic vanadium(IV) species,

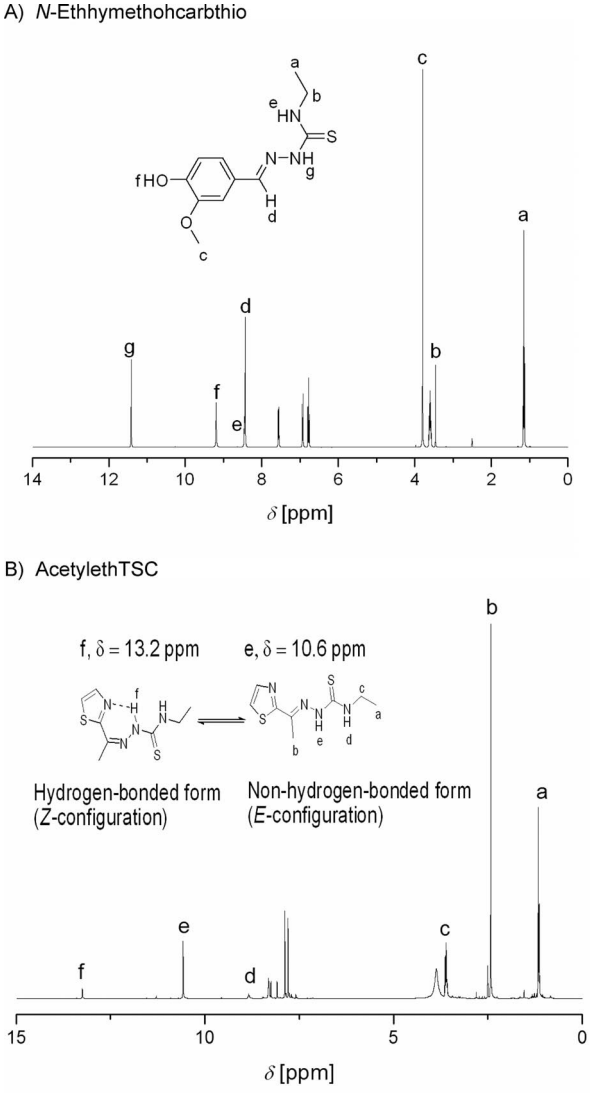

Figure 3. ^{1}H NMR spectra of *N*-ethhymethohcarbthio and acetylethTSC in [D_6]DMSO.

which could be due to vanadium(IV) species that are in equilibrium with vanadium(V) species that are formed upon aerial oxidation in DMSO.

The ^{1}H NMR spectrum of the oxidised product isolated from **1** exhibited resonance signals that are due to aromatic protons in the δ = 7.06–7.52 ppm region. The ^{1}H NMR spectra of the oxidised products isolated from **1** and **3** exhibited resonance signals in the δ = 7.82–8.09 and 7.06 to 10.43 ppm regions, respectively. These resonance signals are assigned to the proton of the azomethine group and the NH proton of the indole ring of the L-tryptophan moiety, respectively. The resonance signal that corresponds to the N2H proton of *N*-ethhymethohcarbthio in the oxidised product isolated from **3** overlaps with the resonance signal assigned to the NH proton of the indole ring of the L-tryptophan moiety. Chemical shifts are observed at δ = 1.17 and 3.79 ppm for the oxidised product isolated from **3**, which are assigned to the methylene and methyl protons of the free *N*-ethhymethohcarbthio, respectively. Signals of aromatic protons are also observed as multiplets in the δ = 6.87–6.96 and 7.00–7.43 ppm ranges. ESI-MS was used to prove the presence of DMSO-containing vanadium(V) complexes, but ^{1}H NMR spectroscopy proved that the chemical shifts for DMSO occur at δ = 2.7 and 3.0–3.6 ppm, which proved the existence of *O*-bonded and *S*-bonded DMSO, respectively.[22] The absence of a peak at δ = 2.7 ppm implies the absence of *O*-bonded DMSO.[22] The resonance due to the presence of an *S*-bonded DMSO produces singlets at δ = 3.36 and 3.34 ppm for the oxidised products isolated from **1** and **3**, respectively.

^{1}H and ^{51}V NMR Spectroscopy of Oxidised Solutions of 1–4 in [D$_6$]DMSO

Over a 24 h period, [D$_6$]DMSO solutions of **1**–**4** were oxidised with the eventual formation of vanadium(V) species. ^{51}V NMR spectroscopy was used to definitively confirm the presence of vanadium(V) species. Figure 4 shows the ^{51}V NMR spectra for [D$_6$]DMSO solutions of **1**–**4** (10 mM) at room temperature, and Table 5 shows the chemical shifts and percentages of species for each vanadium(V) species. It is interesting that two species are formed on oxidation of **1**, **2** and **4**, whereas three species are formed by **3**. It is possible that a mononuclear species is formed in the range δ = –480.5 to –467.7 ppm, based on the chemical shifts obtained for ^{51}V NMR spectra of vanadate(V) esters of monoionised and diionised aromatic 1,2-diols.[23] For example, [VO(gsal)(HL^1)], [VO(asal)(HL^1)] and [VO(vsal)(HL^1)] (gsal, asal and vsal = diionised salicylaldimine of L-glycine, L-alanine and L-valine; HL^1 = catecholate) have chemical shifts of δ = –460, –457 and –455 ppm, respectively, when [D$_6$]DMSO was used as the solvent.

Mauyra et al.[24] have reported the synthesis of new oxidovanadium(V) complexes [VOL(hq)] by the reaction of [VO(acac)$_2$] with LH$_2$ {LH$_2$ = the dibasic tridentate ONO Mannich base [(*S*)-H$_2$glysal, (*S*)-H$_2$alasal, (*S*)-H$_2$leusal and (*S*)-H$_2$ileusal; *S* represents the *S*-enantiomer] obtained by the reduction of the Schiff bases of salicylaldehyde (sal) and the amino acids: glycine (gly), D,L-alanine (ala), leucine (leu) and isoleucine (ileu), respectively} in the presence of 8-hydroxyquinoline (Hhq). Spectroscopic studies were used to confirm that the complexes have octahedral structures.[24] The complexes exhibited a single ^{51}V NMR signal (with [D$_6$]DMSO as solvent) in the range δ = –464.6 to –468.0 ppm due to the existence of a single isomer in solution.[24] Due to the similar chemical shifts of the species in the δ = –480.46 to –467.69 ppm range, we can conclude that a mononuclear vanadium(V) species is formed when the vanadium(IV) complexes are oxidised in [D$_6$]DMSO. The reason why the vanadium(V) species that is formed from **3** has a chemical shift of δ = –467.7 ppm is yet to be determined.

Mauyra et al.[24] carried out a time-dependent ^{51}V NMR spectroscopic study (in [D$_7$]DMF and CD$_3$OD) in order to investigate possible isomerisation and/or further reaction in solution. Freshly prepared solutions of [VO(*S*-alasal)(hq)] showed a signal at δ = –466.7 ppm. As time elapsed, a second, broader signal at δ = –516.3 ppm formed, which had about the same integral intensity as the δ = –466.7 ppm signal after three days and about twice its intensity after one week. The authors concluded that the change in chemi-

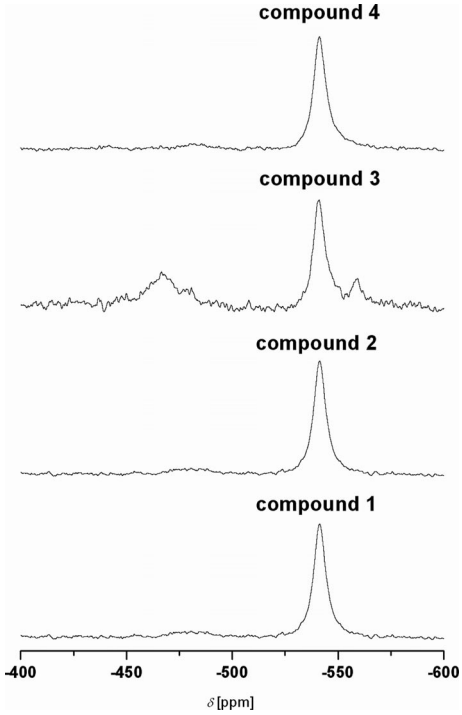

Figure 4. ^{51}V NMR spectra of **1**–**4** after oxidation in [D$_6$]DMSO for 24 h.

Table 5. ^{51}V NMR chemical shifts δ [ppm] and percentages of species of [D$_6$]DMSO solutions for **1**–**4** after being oxidised for 24 h.

	δ	Species (%)	δ	Species (%)	δ	Species (%)
1	–480.5	7.1	–541.4	92.9		
2	–481.9	9.2	–542.2	90.8		
3	–467.7	41.7	–541.0	47.9	–559.3	10.4
4	–481.9	6.9	–541.2	93.1		

cal shift was too large to represent diastereomers based on pairs of enantiomers, and therefore, assigned the new signal to a $[VO_2]$ or $[(VO)_2\mu\text{-}O]$ species, i.e. the oxygenated product after a slow loss of 8-hydroxyquinoline. They also concluded that, as the generation of a $[(VO)_2\mu\text{-}O]$ species usually dominates during oxygenation[24] in the absence of a base, the signal at δ = –516.3 ppm is most probably due to the $[(VO)_2\mu\text{-}O]$ species. In our case, the chemical shift at approximately δ = –541 ppm accounts for the major species formed for **1**–**4**. We believe that this due to $[V_2O_3$(sal-L-tryp$)_2$(DMSO$)_2]$, which was also detected by ESI-MS (*m*/*z* = 918.3, $[V_2O_3$(sal-L-tryp$)_2$(DMSO$)_2$ + H$]^+$) from oxidised DMSO solutions of **1** and **3**. A similar complex with *N*-salicylidene-L-alaninate (sal-L-ala) as a ligand, $[V_2O_3$(sal-L-ala$)_2]\cdot 2CH_2Cl_2$, has been reported by Nakajima et al.[25]

We believe that [VO(sal-L-tryp)([D$_6$]DMSO)(OH)] was formed as an intermediate when **2** and **4** were oxidised in [D$_6$]DMSO, within experimental errors in the determination of the percentage species. We believe that the species with a chemical shift at δ = –559.3 ppm is mononuclear and propose its structure as that shown in Scheme 1 and its formula as [VO(sal-L-tryp)(DMSO)(*N*-ethhymethohcarbthio)]. Based on ^{51}V NMR spectroscopy, we propose the existence of an equilibrium between mononuclear and binuclear vanadium(V) species (Scheme 1).

Based on ^{1}H NMR spectroscopy (Figures S27–S30), it appears as if the thiosemicarbazone ligands became free when **2**–**4** were oxidised in [D$_6$]DMSO and DMSO. The ^{1}H NMR spectroscopic chemical shifts of the free ligands are similar to the values shown in Figure 3 and those obtained for MeATSC.[6] ESI-MS also proved the existence of a free thiosemicarbazone ligand for a mixture that resulted from the oxidation of **3** in DMSO. An *m*/*z* of 252.3 accounted for the presence of free *N*-ethhymethohcarbthio.

UV/Vis and Fluorescence Spectroscopy of 1–4

UV/Vis spectra were acquired for **1**–**4** in DMSO (Figures S31–S34), and the assignments of the absorption bands are shown in Table 6. Charge transfer bands in the 266–292 nm region, which can be assigned to π→π* transitions associated with the thioamide moiety, are observed for **2**–**4**.[18a,26] These occurred at 266 and 292 nm (shoulder) for **2**, 270 and 288 nm (both shoulders) for **3** and 276 nm for **4**. Charge transfer bands assigned to n→π* transitions of aromatic rings are observed in the 316–352 nm region[18a,19a,26–27] and are observed as a shoulder at 316 nm for **2**, at 330 nm for **3**, and 352 nm for **4**.

In the UV region, oxidovanadium(IV) complexes derived from salicylaldehyde generally possess a low-energy band at around 375 nm, which can be attributed to a π→π* transition that originates mainly from the azomethine chromophore.[11] This occurs at 388 nm for **2**, as a shoulder at 390 nm for **3** and hidden under the n→π* transitions at 352 nm for **4**. A band in the 550–558 nm region is assigned to ligand-to-metal charge transfer (LMCT) transitions of the type p→d where p and d represent the lone pair of the phenolato oxygen atom and vanadium 3d orbitals, respectively.[28] This occurs at 558 nm for **1**, 550 nm for **2** and 558 nm for **4**. A similar band is absent for **3** but we believe it to be hidden under the band at 614 nm, which is assigned to d→d transitions.

Table 6. UV/Vis spectroscopic data for **1**–**4**.

	λ [nm]	ε [M^{-1} cm^{-1}]	Assignment
1	558	44	LMCT (p→d transition)
	758	27	d→d transition
2	266	74835	π→π* (thioamide moiety)
	292 (sh)	17954	π→π* (thioamide moiety)
	316 (sh)	10046	n→π* (aromatic rings)
	388	15013	π→π* (azomethine chromophore)
	550	54	LMCT (p→d transition)
	592 (sh)	45	d→d transition
	756	28	d→d transition
3	270 (sh)	10984	π→π* (thioamide moiety)
	288 (sh)	13874	π→π* (thioamide moiety)
	330	24837	n→π* (aromatic rings)
	390 (sh)	18250	π→π* (azomethine chromophore)
	620	852	d→d transition
4	276	21969	π→π* (thioamide moiety)
	352	14227	n→π* (aromatic rings)
	558	80	LMCT (p→d transition)
	590 (sh)	70	d→d transition
	756	38	d→d transition

Bands assigned to d→d transitions were also observed in the 756–758 nm region for **1**, **2** and **4**.[19b] This occurred at 758 nm for **1** and 756 nm for **2** and **4**. In the electronic spectra of **2** and **4**, bands at 592 nm for **2** and 590 nm for **4** are also assigned to d→d transitions and appear as shoulders of the much stronger LMCT band in the 550–558 nm region.[19b]

Fluorescence spectra were acquired for **2**–**4** in DMSO (Figures S35–S37). The excitation wavelengths for **2**, **3** and **4** were 400, 330 and 340 nm, respectively. Compound **2**, which contains an anthracene unit in MeATSC, produced the highest intensity in its fluorescence spectra, whereas **3** and **4** produced lower intensities.

ESR Spectroscopy

Compounds **1**–**4** were also characterised by low-temperature ESR spectroscopy and each complex exhibits a powder-type axial g = 2 signal (S = 1/2) with a minor rhombic distortion at 10 K. The observed hyperfine structure shows sixteen line ESR signals with partial overlap of three lines. Figure 5 shows two representative ESR spectra along with simulations for **1** and **4**. These spectra are characteristic of slowly tumbling macromolecular complexes consistent with vanadyl (VO^{2+})-containing complexes, which indicates that the vanadium centre has a +4 oxidation state in the two freshly prepared complexes. The sixteen lines seen in the anisotropic powder ESR spectra are due to the hyperfine interaction between the electron spin and the nuclear spin of $^{51}V^{IV}$ (I = 7/2, 100% natural abundance).

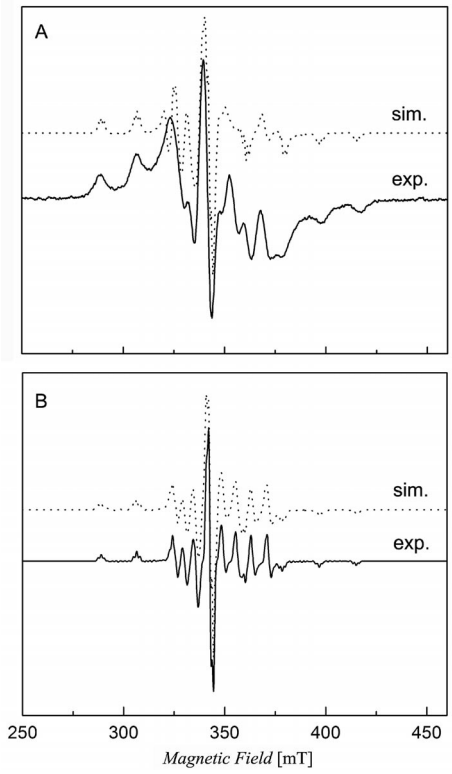

Figure 5. X-band continuous-wave ESR spectra of **1** (A, 10 mM in DMSO) and **4** (B, 10 mM in DMSO) overlaid with spectral simulations.

The powder ESR spectra of **1**–**4** were simulated to determine the magnitudes of the principal ^{51}V hyperfine coupling constants (A_x, A_y, and A_z) and g values using the ESR simulation program DOUBLET.EXE.[29] The ESR parameters obtained from spectral simulations are shown in Table 7. The large A values and broad linewidth are presumably due to the sulfur ligation and hexacoordinate geometry. The vanadyl cation, VO^{2+}, is known to form complexes that are pentacoordinate or square bipyramidal with a short V=O bond,[30] and few hexacoordinate vanadyl-containing complexes with mixed N,O,S ligands have been characterised to date. The ESR spectra of the complexes described here may be useful in future studies of VO^{2+} in complexes and biological systems. Nevertheless, these ESR spectroscopic results are in agreement with those of UV/Vis and FTIR spectroscopy and thus prove that each synthesised compound has a vanadium(IV) centre prior to aerial oxidation of the DMSO solution. We plan to carry out studies that involve DFT calculations to elucidate the dependence of calculated ^{51}V A_z values on the orientation and geometry of the coordinated thiosemicarbazone and water ligands in **1**–**4**. Such a study that involves calculated and experimental A_z values for **1**–**4** would complement the excellent data for $V^{IV}O$ complexes that have been reported by Garriba and coworkers.[31]

Table 7. ESR parameters of **1**–**4**.[a]

	g_x	g_y	g_z	A_x	A_y	A_z
1	1.958	1.988	1.953	80	68	180
2	1.98	1.98	1.968	64	65	178
3	2	1.995	1.965	63	63	175
4	1.98	1.98	1.968	64	65	178

[a] ESR parameters were obtained from spectral simulations as described in the text.

Pharmacology

In Vitro Cytotoxicity

The objective of this research was to evaluate the antiproliferative activity of **2**–**4** against colon cancer cell lines (HTC-116, Caco-2 and HT-29) and to compare the antiproliferative activity against one noncancerous colon cell line (CCD-18Co). Compounds **2**–**4**, cisplatin and etoposide were evaluated for their cytotoxicity against HCT-116, Caco-2 and HT-29 by a colorimetric assay (MTS), which measures mitochondrial dehydrogenase activity as an indication of cell viability. The effects of the compounds on the viability of these cells were evaluated after continuous incubation (24, 48 and 72 h).

The growth inhibition effects of the compounds were investigated in noncancerous colonic myofibroblast CCD-18Co cells and compared to the colon cancer cell lines. The results demonstrated a great difference in the inhibition of cell proliferation between cancer lines and the noncancerous CCD-18Co cells. Compounds **2**–**4** have been shown to decrease the cell viability of HCT-116, Caco-2 and, more potently, HT-29 cells (Table 8). Compound **4** was the most active of the three tested, whereas **2** and **3** showed similar activities in both cancer cell lines. Figure 6 shows a plot of percentage cell viability vs. concentration of **4** against the HT-29 cancer cell line, and Table 8 shows the IC_{50} values for the inhibition of cell proliferation for **2**–**4**, with IC_{50} values generally around 100 μM concentration at 72 h in **2** and **3**. None of the compounds had better a efficacy against any of the cancer cell lines than etoposide. Compound **4** had a better efficacy against the HT-29 cancer cell line than cisplatin (Table 8).

Compounds **2**–**4** exhibited lower inhibitory effects in normal human CCD-18Co cells, which indicates a possible cytotoxic selectivity towards colon cancer cells (Table 8). IC_{50} values in CCD-18Co were around three and two times greater than those in HT-29 and Caco-2 and HCT-116, respectively. However, the cytotoxic selectivity towards cancer colon cells of cisplatin (as a positive control) was slightly lower, except with Caco-2 cells (Table 8). These results are in good agreement with those of a previous study, where it was shown that cisplatin inhibited cell proliferation by about 70% in both cell lines (cancer and normal colon cells).[32] In general, **2**–**4**, which have been proven to be growth suppressors of cancer cells but do not affect noncancerous cells, may have a potential in chemotherapy.

Although metal complexes are being investigated as probes and therapeutics, there have been relatively few studies on their mechanism of uptake. Metal complexes that are lipophilic cations may passively diffuse across the plasma

Table 8. Antiproliferative effects of **2**–**4**, cisplatin and etoposide on different cells lines after 24, 48 and 72 h treatment. Data are expressed as IC_{50} (μM). IC_{50} is defined as the concentration required to achieve 50% inhibition over control cells (0.5% DMSO); IC_{50} values are shown as mean standard error values taken from three independent experiments.

	HT-29			Caco-2		
	24 h IC_{50} [μM]	48 h IC_{50} [μM]	72 h IC_{50} [μM]	24 h IC_{50} [μM]	48 h IC_{50} [μM]	72 h IC_{50} [μM]
2	277.1 ± 10.2	239.6 ± 7.9	100.3 ± 5.1	349.1 ± 19.5	277.1 ± 16.3	147.1 ± 10.8
3	244.2 ± 8.8	169.6 ± 15.1	87.9 ± 0.5	367.0 ± 21.5	281.6 ± 14.4	152.5 ± 12.7
4	128.6 ± 10.7	82.4 ± 9.6	47.8 ± 5.5	242.1 ± 25.1	166.2 ± 15.3	85.4 ± 14.0
Cisplatin	84.7 ± 1.9	80.6 ± 1.6	69.1 ± 3.2	32.0 ± 1.6	22.8 ± 1.5	17.9 ± 1.8
Etoposide	19.2 ± 0.8	17.3 ± 1.9	15.8 ± 2.4	47.6 ± 0.8	46.2 ± 1.9	40.9 ± 1.5
	HCT-116			CCD-18Co		
	24 h IC_{50} [μM]	48 h IC_{50} [μM]	72 h IC_{50} [μM]	24 h IC_{50} [μM]	48 h IC_{50} [μM]	72 h IC_{50} [μM]
2	203.4 ± 7.7	181.3 ± 9.2	115.0 ± 6.5	495.6 ± 23.5	339.2 ± 16.7	208.0 ± 11.9
3	227.4 ± 6.8	192.7 ± 11.6	110.3 ± 10.1	490.6 ± 27.6	329.5 ± 15.4	203.6 ± 12.5
4	161.3 ± 4.6	134.9 ± 3.9	89.5 ± 14.5	382.7 ± 21.9	246.2 ± 11.4	152.2 ± 12.0
Cisplatin	53.8 ± 2.1	49.7 ± 1.3	41.0 ± 2.7	83.0 ± 1.1	72.0 ± 1.5	64.1 ± 1.6
Etoposide	40.8 ± 0.5	36.2 ± 2.0	38.4 ± 1.2	82.5 ± 3.1	79.2 ± 1.2	73.2 ± 1.9

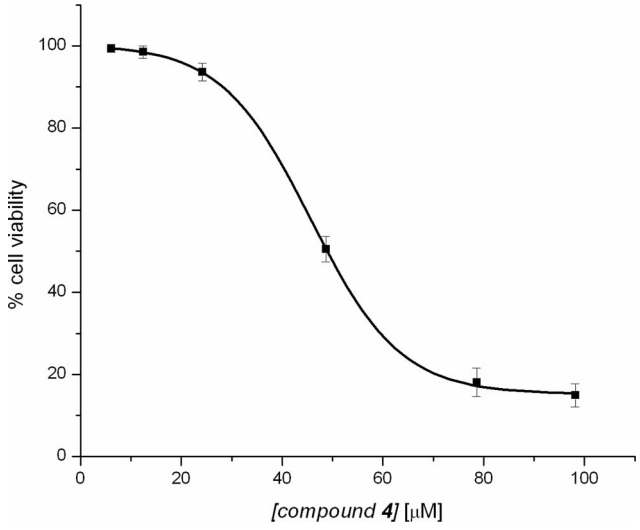

Figure 6. MTT cell proliferation assay of **4** against the HT-29 cancer cell line.

membrane in response to the membrane potential.[33] A ruthenium(II) complex that contained the lipophilic 4,7-diphenyl-1,10-phenanthroline ligand has been shown to enter the membrane by passive diffusion in a membrane-potential dependent manner.[33] It is believed that the excellent efficacy of ruthenium(II) complexes with thiosemicarbazones, which have been reported by Beckford and coworkers,[6] is likely due to the fact that the complexes are lipophilic cations. As a point of speculation, this may explain why cations such as $[(bpy)_2Ru(TSC)]^{2+}$ and $[(phen)_2Ru(TSC)]^{2+}$ (TSC = 9-anthraldehydethiosemicarbazones)[6] have better efficacies against HT-29 and HCT-116 cell lines vs. our neutral vanadium(IV) complexes. Based on ^1H NMR spectroscopy and ESI-MS studies where the free ligand was observed, we believe that the free ligand likely causes the cell death as opposed to the vanadium species. In order to prove this belief, we will have to carry out in vitro studies with the free ligands. A systematic study will have to be carried out with the ruthenium(II) complexes and **2**–**4** under the same conditions. Apart from such a study, a more detailed emphasis will be placed on the methods used to examine cellular accumulations to identify the mechanism(s) of uptake, and to monitor possible efflux of **2**–**4** and their analogues.

Conclusions

Two new thiosemicarbazone and three new vanadium(IV) complexes with mixed ligands were successfully synthesised and characterised. The anticancer properties of **2**–**4** were examined with three colon cancer cell lines, HTC-116, Caco-2 and HT-29, along with a comparative antiproliferative study on noncancerous colonic myofibroblasts, CCD-18Co. Compounds **2** and **3** exhibited a less inhibitory effect in human noncancerous CCD-18Co cells, which indicates a possible cytotoxic selectivity towards colon cancer cells. In general, the compounds that exhibited antiproliferative activity on cancer cells but did not affect noncancerous colorectal cells may have a potential in chemotherapy.

Experimental Section

Materials and Methods: Analytical or reagent grade chemicals were used throughout. All the chemicals, including solvents, were obtained from Sigma–Aldrich (St. Louis, MO, USA) or other commercial vendors, and used as received. Microanalyses (C, H, N) were performed by Desert Analytics, Tucson, USA and Columbia Analytical Services 3860 S. Palo Verde Road Suite 303 Tucson, AZ 85714, USA. ^1H and ^{13}C NMR spectra were acquired in $[D_6]$-DMSO with JEOL ECX-300, Varian 300 MHz, Bruker 400 MHz and Varian 500 MHz spectrometers at room temperature. The residual ^1H and ^{13}C present in $[D_6]$DMSO (2.49 and 39.7 ppm, respectively) were used as internal references. ^{51}V NMR spectra were acquired with a Varian 500 MHz spectrometer with $[D_6]$-DMSO as solvent and $VOCl_3$ as an external reference as described for vanadium(V) compounds.[34] ESR spectra were acquired at 10 or 20 K with a Bruker ER200D spectrometer with a 4116DM reso-

nator. The sample temperature was maintained with a temperature controller (ITC503S), an ESR910 liquid helium cryostat and LLT650/13 liquid helium transfer tube (Oxford Instruments, Concord, MA, USA). Instrument conditions were as follows, modulation frequency: 100 kHz, modulation amplitude: 0.3 G, microwave frequency: 9.64 GHz and microwave power: 0.004 mW. FTIR spectra were acquired in the 4000–400 cm^{-1} range using an ATR accessory (with a diamond crystal) with a Nicolet 6700 FTIR spectrophotometer. Electronic spectra were acquired with quartz cuvettes with a HP8452 diode array spectrophotometer using DMSO as the solvent. Fluorescence spectra were acquired with a Cary Eclipse fluorescence spectrophotometer (Varian Inc.) with a slit width of 10 nm. ESI-MS were acquired with an HP Agilent 1956b single-quadrupole mass spectrometer. Samples were dissolved in an acetic acid/methanol mixture and the solution was introduced by direct injection using a syringe pump with a flow rate of 100 $\mu L\,s^{-1}$ while sweeping the cone voltage from 0 to 200 V at a rate of 10 $V\,min^{-1}$. All *m*/*z* ratios and percentages were determined by using MestReNova software.

X-ray Crystallography: Crystallographic data were collected at T = 90 K with a Bruker Kappa Apex-II CCD diffractometer equipped with Cu-K_α radiation and an Oxford Cryosystems Cryostream cooler. The structure of acetylethTSC was solved using SHELXS[35] and refined using the SHELX97[36] software packages. All H atoms were visible in difference maps. Coordinates of the NH hydrogen atoms were refined individually, whereas those on C were placed in idealised positions, with torsional parameters refined for the methyl groups.

Crystal data: $C_8H_{12}N_4S_2$, FW = 228.34, monoclinic, space group = *C*2/*c*, a = 10.4549(10), b = 10.8970(10), c = 18.7694(15) Å, β = 91.544(5)°, V = 2137.6(3) $Å^3$, Z = 8, T = 90.0(5)K, μ = 4.25 mm^{-1}, d_{calc} = 1.419 $g\,cm^{-3}$, colourless parallelepiped, dimensions = 0.18 × 0.17 × 0.09 mm, reflections collected: 8017, unique reflections = 1901, observed reflections [$I > 2\sigma(I)$] = 1738, R_{int} = 0.026, no. of parameters: 136, R_1 = 0.028, wR_2 = 0.069, GOF(F^2) = 1.065.

CCDC-812348 contains the supplementary crystallographic data for this paper. These data can be obtained free of charge from The Cambridge Crystallographic Data Centre via www.ccdc.cam.ac.uk/data_request/cif.

Synthesis of Ligands

9-Anthraldehydethiosemicarbazone (ATSC) and 9-anthraldehyde-*N*(4)-methylthiosemicarbazone (MeATSC) were prepared according to the procedure by Beckford et al.[6]

Synthesis of *N*-Ethhymethohcarbthio: *o*-Vanillin (3.00 g, 19.7 mmol) and 4-ethyl-3-thiosemicarbazide (2.35 g, 19.7 mmol) were placed in a 250 mL round-bottomed flask followed by absolute ethanol (100 mL). Glacial acetic acid (approx. 10 drops) was added to the off-white suspension, and the reaction mixture was heated to reflux for 3 h. The reaction mixture was cooled to room temperature and filtered through a sintered glass crucible. The white residue was washed with ethanol (3 × 15 mL) and ether (3 × 10 mL) and allowed to air dry; yield 4.97 g (99%). $C_{10}H_{13}N_3O_2S$ (239.29): calcd. C 52.15, H 5.97, N 16.59; found C 52.53, H 6.16, N 17.02. FTIR: $\tilde{\nu}$ = 3304 (m) (N^1H), 3300 (m) (N^2H), 3130 (br.) (OH), 1155 (m) (N–N), 1606 (m) [TSC (C=N)], 1267 (m) and 831 (m) (C=S) cm^{-1}. ^1H NMR (400 MHz, [D_6]DMSO): δ = 1.15 (t, J^t = 7.10 Hz, 3 H, CH_3), 3.46 (s, 1 H, CH_3OAr), 3.60 (q, 2 H, CH_2), 3.80 [s, 1 H, (azomethine CH=N)], 6.79 (t, J^t = 7.95 Hz, CH_{ar}), 6.96 (dd, J^{dd} = 1.49 and 8.06 Hz, CH_{ar}), 7.55 (dd, J^{dd} = 1.51 and 7.93 Hz, CH_{ar}), 8.40 (s, H, aminic-NH), 11.41 (s, 1 H, ArOH), and 11.42 (s, 1 H, hydrazinic-NH) ppm. ^{13}C NMR (400 MHz, [D_6]DMSO): δ = 176.86 (C=S), 147.86 (CH=N), 145.88 ($COCH_{3ar}$), 139.00 (PhOH), 120.82 ($CCH=N_{ar}$), 118.91 (CH_{ar}), 118.10 (CH_{ar}), 112.66 (CH_{ar}), 58.85 (OCH_3), 38.28 (CH_2), 14.60 (CH_3) ppm.

Synthesis of AcetylethTSC: 2-Acetylthiazole (0.636 g, 0.518 mL 5.0 mmol) was placed in a 100 mL round-bottomed flask followed by anhydrous methanol (25 mL). 4-Ethyl-3-thiocarbazide (0.596 g, 5.0 mmol) in anhydrous methanol (25 mL) was slowly added to the solution followed by a few drops of concentrated hydrochloric acid. The reaction mixture was heated to reflux with stirring for 2 h and then evaporated to a minimum volume to form a yellow solid. The residue was collected by filtration, washed with diethyl ether and air-dried; yield 0.750 g (66%). A single crystal for X-ray crystallography was grown by slow evaporation of a methanol solution. FTIR: $\tilde{\nu}$ = 3164 (m) (N^1H), 3054 (m) (N^2H), 1059 (m) (NN), 1543 (m) [TSC (C=N)], 1296 (m) and 813 (m) (C=S) cm^{-1}. ^1H NMR (400 MHz, [D_6]DMSO): δ = 1.16 (t, J^t = 7.10 Hz, 3 H, CH_3), 2.42 (s, 3 H, $CH_3CH=N$), 3.61 (d, 2 H, CH_2), 7.79 (d, J^d = 3.21 Hz, CH_{ar}), 7.88 (d, J^d = 3.19 Hz, CH_{ar}), 8.08 (d, J^d = 3.24 Hz, CH_{ar}), 8.30 (s, H, aminic NH), 10.58 (s, 1 H, hydrazinic-NH), 13.2 (s, *H*-bonded hydrazinic NH) ppm.

Synthesis of the Reduced Schiff Base 2-(2-Hydroxybenzylamino)-3-(1*H*-indol-3-yl)propanoic Acid: The reduced Schiff base was prepared by a known procedure that involved salicylaldehyde, amino acids, and $NaBH_4$, but with L-tryptophan using the following procedure:[10] L-Tryptophan (2.04 g, 10.0 mmol) and potassium hydroxide (0.56 g, 10.0 mmol) were added to a 125 mL Erlenmeyer flask followed by deionised water (10 mL). Salicylaldehyde (1.029 mL, 10.0 mmol) in absolute ethanol (10 mL) was slowly added to the mixture. The yellow solution was stirred for 30 min prior to cooling in an ice bath. The intermediate Schiff base that was produced in situ was reduced with an excess of sodium borohydride (0.46 g, 12 mmol) in water (5 mL) that contained NaOH solution (10 drops, 2 M). The solution was stirred for 10 min, and the yellow colour slowly faded. The solution was acidified with concentrated HCl to pH 4.68. The resulting solid was collected by filtration, washed with ethanol (2 × 30 mL) and diethyl ether (2 × 30 mL) and dried. The white solid was recrystallised twice from water/ethanol (1:1); yield 1.08 g (35%). ESI-MS (+ve mode): *m*/*z* (%) = 311.08 (100.00, [M + H]$^+$), 242.42 (13.04, [M – CHO_3 + H]$^+$), 620.36 (12.77, [2M + H]$^+$), 930.39 (5.02, [3M + H]$^+$), 1240.92 (3.92, [4M + H]$^+$). FTIR: $\tilde{\nu}$ = 3392 (m) (indolic NH), 3055 (br.) (OH), 1208 (m) (C–O), 1494 (m) (COO_s) and 1592 (m) ($CO-O_{as}$) cm^{-1}. ^1H NMR (400 MHz, [D_6]DMSO): δ = 2.67 (d, 2 H), 3.21 (d, 2 H), 3.05 (d, 2 H), 5.91 (t, 1 H), 6.15 (d, 1 H), 6.31 (d, 1 H), 6.62 (m, 1 H), 6.62 (m, 1 H), 6.62 (m, 1 H), 6.62 (m, 1 H), 6.90 (d, 1 H) and 7.18 (d, 1 H) ppm. ^{13}C NMR (400 MHz, [D_6]DMSO): δ = 28.57, 46.72, 63.61, 110.66, 111.57, 113.46, 118.50, 118.69, 121.37, 123.85, 123.89, 126.95, 127.78, 128.16, 128.34, 135.97, 164.55, 182.05 ppm.

Synthesis of K[(sal-L-tryp)]: K[(sal-L-tryp)] was prepared using a method reported by Vanco et al.[37] To a mixture of L-tryptophan (3.07 g, 15.0 mmol) and potassium hydroxide (0.85 g, 15.0 mmol) dissolved in water (5 mL) was added a solution of salicylaldehyde (1.57 mL, 15.0 mmol) in ethanol (10 mL) with stirring. The resulting yellow solution was stirred at room temperature for 24 h before it was diluted by ethanol (25 mL). Upon slow evaporation of solvent, a yellow oil was formed, which was triturated with diethyl ether. The yellow powder was collected by filtration and dried under vacuum; yield 4.85 g (93%). ESI-MS (+ve mode): *m*/*z* (%) = 344.05 (39.65, [M + H]$^+$), 300.03 (100.00, [M – OH – K + H]$^+$), 281.14 (46.08, [M – OH – O – K + H]$^+$), 262.12 (1.51, [M – COO – K + H]$^+$), 242.62 (64.65, [M – COO – OH – K + H]$^+$), 205.20

(50.43, [M – C_7H_6O – K + H]$^+$). FTIR: $\tilde{\nu}$ = 3407 (m) (indolic NH), 3169 (br.) (OH), 1194 (m) (C–O), 1521 (m) (COO_s), 1604 (m) (COO_{as}), 1570 (m) [TSC (C=N)] cm^{-1}. ^{1}H NMR (400 MHz, [D_6]-DMSO): δ = 3.13 (dd, J^{dd} = 8.9 and 16 Hz, 2 H), 3.49 (s, 1 H), 4.07 (s, 1 H), 6.59 (s, 1 H), 6.72–7.06 (m, 1 H), 6.72–7.06 (m, 1 H), 7.20 (s, 1 H), 7.20 (m, 1 H), 7.20 (m, 1 H), 7.20 (m, 1 H), 7.35–7.58 (m, H), 7.35–7.58 (m, 1 H), 11.17 (s, 1 H) ppm. ^{13}C NMR (400 MHz, [D_6]DMSO): δ = 30.16, 64.82, 72.43, 111.39, 111.56, 115.74, 117.62, 117.99, 118.31, 118.33, 120.59, 123.38, 127.36, 131.77, 132.01, 163.27, 172.88 ppm.

Synthesis of [VO(sal-L-tryp)(H_2O)] (1): Complex **1** was prepared as described by Costa Pessoa et al.[11] L-Tryptophan (1.14 g, 5.60 mmol) and sodium acetate trihydrate (1.47 g, 10.8 mmol) were placed in a 250 mL round bottomed flask with deionised water (100 mL). The mixture was stirred and heated at 50 °C to completely dissolve the L-tryptophan. Salicylaldehyde (0.59 mL, 5.6 mmol) in absolute ethanol (14 mL) was slowly added to the mixture. The resulting yellow solution was stirred vigorously with a magnetic stirrer, and an aqueous solution of $VOSO_4{\cdot}xH_2O$ (0.78 g, 4.8 mmol) in water (2 mL) was added dropwise to the solution and it was stirred for 30 min. A dark brown precipitate formed, and the resulting solution was filtered under vacuum. The grey solid collected was washed with water (30 mL) and an ethanol/water mixture (50:50, 30 mL) and air-dried; yield 1.19 g (63%). $C_{18}H_{16}N_2O_5V$ (391.28): calcd. C 55.25, H 4.12, N 7.16; found C 55.16, H 4.31, N 6.87 (ref.[11] $C_{18}H_{16}N_2O_5V$: calcd. C 55.25, H 4.12, N 7.16; found C 55.2, H 4.2, N 7.1). FTIR: $\tilde{\nu}$ = 3478 (m) (indolic NH), 3014 (br.) (OH), 1540 (m) (C–O), 1490 (m) (COO_s), 1597 (m) (COO_{as}), 1600 (m) {[(sal-L-tryp)] C=N}, 997 (s) (V=O) cm^{-1} [ref.[11] 3480 (m) (indolic NH), 3065 (br.) (OH), 1630 (m) {[(sal-L-tryp)] (C=N)}, 1600 (m) (C–O), 970 (s) (V=O) cm^{-1}]. UV/Vis (MeOH): $\lambda_{max.}$ (ε/M^{-1} cm^{-1}) = 558 (44) and 758 (27) nm [ref.[11] (DMSO) 275 (15400) and 375 (4850), 520 (45), and 730 (20) nm].

Synthesis of [VO(sal-L-tryp)(MeATSC)]·1.5C_2H_5OH (2): (*E*)-2-(Anthracen-9-ylmethylene)-*N*-methylhydrazinecarbothioamide (0.15 g, 0.51 mmol) and **1** (0.20 g, 0.51 mmol) were placed in a dry 250 mL round-bottomed flask. Absolute ethanol (100 mL) was added to the flask, and the solution was heated to reflux with stirring under argon for 2 h. The orange-blue solution was evaporated to dryness. Diethyl ether was added, the mixture was filtered under vacuum, and the green residue was collected and air-dried; yield 0.23 g (68%). $C_{38}H_{38}N_5O_{5.5}SV$ (735.75): calcd. C 62.03, H 5.21, N 9.52; found C 62.62, H 5.25, N 9.33. ESI-MS: *m*/*z* (%) = 666.17 (100.00, [M + H]$^+$), 577.08 (33.10, [M – $C_2H_5N_2S$ + H]$^+$), 405.14 (31.86, [M – $C_{17}H_{17}N_3$ + H]$^+$), 292.14 (54.60, [MeATSC + H]$^+$). FTIR: $\tilde{\nu}$ = 3308 (m) (indolic NH), 3340 (m) (N^1H), 2976 (m) (N^2H), 1148 (m) (N–N), 1544 (m) (C–O), 1491 (m) (COO_s), 1600 (s) (COO_{as}), 1624 (m) [TSC (C=N)], 1590 (m) {[(sal-L-tryp)] (C=N)}, (1225) (m), (829) (m) (C=S), (455) (m) (V–S), 980 (s) (V=O) cm^{-1}. UV/Vis (DMSO): $\lambda_{max.}$ (ε/M^{-1} cm^{-1}) = 226 (74835), 292 (sh) (17954), 316 (sh) (10046), 388 (15013), 550 (54), 592 (sh) (45), 756 (28) nm.

Synthesis of [VO(sal-L-tryp)(*N*-ethhymethohcarbthio)]·H_2O (3): Complex **3** was prepared in a similar manner to **2** from (*E*)-2-(4-hydroxy-3-methoxybenzylidene)-*N*-methylhydrazinecarbothioamide (0.065 g, 0.26 mmol) and **1** (0.10 g, 0.26 mmol); yield 0.12 g (78%). $C_{29}H_{30}N_4O_7SV$ (629.58): calcd. C 53.33, H 4.64, N 11.11; found C 53.18, H 5.21, N 11.09. ESI-MS: *m*/*z* (%) = 624.87 (100.00, [M – H]$^-$), 431.90 (64.75, [M – $C_{11}H_{10}N_2O$ – H]$^-$), 407.85 (20.99, [M – $C_{11}H_{15}N_3O_2S$ – H]$^-$), 287.88 (12.70, [$C_{11}H_{15}N_3O_2S$ – C_8H_7N – H]$^-$), 252.00 (25.74, [*N*-ethhymethohcarbthio – H]$^-$). FTIR: $\tilde{\nu}$ = 3210 (m) (indolic NH), 3306 (m) (N^1H), 2970 (m) (N^2H), 3010 (br.) (OH), 1154 (m) (N–N), 1540 (m) (C–O), 1480 (m) (COO_s), 1600 (s) (COO_{as}), 1620 (m) [TSC (C=N)], 1580 (m) {[(sal-L-tryp)] (C=N)}, (1270) (m), (802) (m) (C=S), (454) (m) (V–S), 976 (s) (V=O) cm^{-1}. UV/Vis (DMSO): $\lambda_{max.}$ (ε/M^{-1} cm^{-1}) = 270 (sh) (10984), 288 (sh) (13874), 330 (24837), 390 (sh) (18250), 620 (852) nm.

Synthesis of [VO(sal-L-tryp)(acetylethTSC)]·C_2H_5OH (4): Complex **4** was prepared in a similar manner to **2** from 2-acetylthiazole-4,4′-dimethylthiosemicarbazone (0.12 g, 0.51 mmol) and **1** (0.20 g, 0.51 mmol); yield 0.18 g (57%). $C_{28}H_{32}N_6O_5S_2V$ (647.66): calcd. C 51.93, H 4.98, N 12.98; found C 52.49, H 4.72, N 10.91. ESI-MS: *m*/*z* (%) = 600.25 (2.71, [M + H]$^+$), 513.57 (100.00, [M – C_3H_7NS + H]$^+$), 482.38 (37.11, [M – C_7H_5NO + H]$^+$), 336.06 (4.13, [M – $C_{17}H_{15}N_2O$ + H]$^+$). FTIR: $\tilde{\nu}$ = 3229 (m) (indolic NH), 3310 (m) (N^1H), 2976 (m) (N^2H), 1149 (m) (N–N), 1545 (m) (C–O), 1480 (m) (COO_s), 1600 (s) (COO_{as}), 1624 (m) [TSC (C=N)], 1580 (m) {[(sal-L-tryp)] (C=N)}, (1287) (m), (819) (m) (C=S), (455) (m) (V–S), 982 (V=O) cm^{-1}. UV/Vis (DMSO): $\lambda_{max.}$ (ε/M^{-1} cm^{-1}) = 276 (21969), 352 (14227), 558 (80), 590 (sh) (70), 756 (38) nm.

Oxidation of 1 and 3 in DMSO: Complex **1** (0.1 g, 0.26 mmol) was added to an evaporating dish with DMSO (10 mL), and the resulting solution was left to evaporate for 32 days to leave a solid; yield 0.09 g. ESI-MS (+ve mode): *m*/*z* (%) = 468.60 (1.67, [M + H]$^+$), 242.41 (100.00, [M – OH – DMSO – C_8H_7N + H]$^+$), 451.05 (48.25, [M – OH + H]$^+$), 763.68 (30.06, [V_2O_3(sal-L-tryp)$_2$ + H]$^+$), 776.77 (49.36, [V_2O_3(sal-L-tryp)$_2$(H_2O) + H]$^+$), 918.28 (3.13, [V_2O_3(sal-L-tryp)$_2$(DMSO)$_2$ + H]$^+$). FTIR: $\tilde{\nu}$ = 3185 (m) (indolic NH), 3194 (br.) (OH), 1551 (m) (C–O), 1497 (m) (COO_s), 1618 (s) (COO_{as}), 1667 (m) [TSC (C=N)], 1581 (m) {[(sal-L-tryp)] (C=N)}, 1164 (m), 1213 (m) (S=O), 949 (s) (V=O) cm^{-1}. ^{1}H NMR (400 MHz, [D_6]DMSO): δ = 2.52 (d, 3 H), 2.52 (d, 3 H), 10.89 (s, 1 H), 7.06 (s, 1 H), 7.22 (m, 1 H), 7.22 (m, 1 H), 7.52 (d, 1 H), 8.06 (d, 2 H), 3.36 (s, 1 H), 3.00 (s, 2 H), 7.22 (m, 1 H), 7.22 (m, 1 H), 7.22 (m, 1 H), 7.22 (m, 1 H), 9.93 (s, 1 H), 7.06 (s, 1 H) ppm.

Complex **3** (0.1 g, 0.16 mmol) was oxidised in an analogous manner; yield 0.09 g. ESI-MS (+ve mode): *m*/*z* (%) = 470.01 (0.50, [M + H]$^+$), 252.26 (100.00, [*N*-ethhymethohcarbthio + H]$^+$), 451.96 (2.97, [M – OH + H]$^+$), 702.75 (2.15, [M – OH + *N*-ethhymethohcarbthio + H]$^+$), 763.22 (0.74, [V_2O_3(sal-L-tryp)$_2$ + H]$^+$), 775.40 (1.08, [V_2O_3(sal-L-tryp)$_2$(H_2O) + H]$^+$), 916.44 (0.75, [V_2O_3-(sal-L-tryp)$_2$(DMSO)$_2$ + H]$^+$). FTIR: $\tilde{\nu}$ = 3193 (br.) (OH), 1666 (m) (C=N), 1600 (C=O), 1550 (m) (C–O), 1133 (m), 1157 (m) (S=O), 946 (s) (V=O) cm^{-1}. ^{1}H NMR (400 MHz, [D_6]DMSO): δ = 2.52 (d, 3 H), 2.52 (d, 3 H), 10.43 (s, 1 H), 6.96 (s, 1 H), 7.22 (m, 1 H), 7.22 (m, 1 H), 7.42 (d, 1 H), 8.00 (d, 2 H), 3.34 (s, 1 H), 3.00 (s, 2 H), 7.22 (m, 1 H), 7.22 (m, 1 H), 7.22 (m, 1 H), 7.22 (m, 1 H), 9.95 (s, 1 H), 6.96 (s, 1 H) ppm.

Pharmacology

Cell Culture: Three human colon cancer cells, HT-29 (human colon adenocarcinoma), HCT-116 (human colon carcinoma) and Caco-2 (human epithelial colorectal adenocarcinoma), and noncancerous human colon cells, CCD-18Co (human colon fibroblasts), were used in this study. All cell lines were obtained from the American Type Culture Collection (ATCC, Rockville, MD, USA) and maintained at the University of Rhode Island, USA. Caco-2 cells were grown in Eagle's minimal essential medium (EMEM) supplemented with 10% v/v fetal bovine serum, 1% v/v nonessential amino acids, 1% v/v L-glutamine and 1% v/v antibiotic solution (Sigma–Aldrich). HT-29 and HCT-116 cells were grown in McCoy's 5a medium supplemented with 10% v/v fetal bovine serum, 1% v/v non-essential amino acids, 2% v/v 4-(2-hydroxyethyl)-1-piperazineethanesulfonic acid and 1% v/v antibiotic solution. CCD-18Co cells were

grown in EMEM medium supplemented with 10% v/v fetal bovine serum, 1% v/v nonessential amino acids, 1% v/v L-glutamine and 1% v/v antibiotic solution and were used from PDL = 26 to PDL = 35 for all experiments. Cells were maintained at 37 °C in an incubator under a 5% CO_2/95% air atmosphere at constant humidity and maintained in the linear phase of growth. The pH of the culture medium was determined with pH indicator paper (pHydrionTM Brilliant, pH 5.5–9.0, Micro Essential Laboratory, NY, USA) inside the incubator. All test samples were dissolved in DMSO (< 0.5% in the culture medium) with sonication and filter sterilised (0.2 μm) prior to addition to the culture media. Control cells were also tested in parallel sequences and subjected to the same changes in medium with 0.5% DMSO.

Cytotoxicity Assay: This assay was carried out as described previously[38] to measure the IC_{50} values for the samples. The in vitro cytotoxicity of the samples was assessed in tumour cells by a tetrazolium-based colorimetric assay, which takes advantage of the metabolic conversion of MTS to a reduced form that absorbs light at 490 nm. Cells were counted using a hemacytometer and were plated at 2000–5000 cells per well, depending on the cell line, in a 96-well format for 24 h prior to drug addition. Test samples and a positive control, etoposide 4 mg mL^{-1} (Sigma–Aldrich), were dissolved in DMSO with sonication. All samples were diluted with media to the desired treatment concentration, and the final DMSO concentration per well did not exceed 0.5%. Control wells were also included on all plates. Following a 24, 48 or 72 h drug-incubation period at 37 °C with serially diluted test compounds, MTS and the electron coupling agent, phenazine methosulfate, were added to the wells, and the cells were incubated at 37 °C in a humidified incubator for 3 h. Absorbances at 490 nm (OD_{490}) were acquired with a spectrophotometer (SpectraMax M2, Molecular Devices Corp., operated by SoftmaxPro v.4.6 software, Sunnyvale, CA, USA) to obtain the number of surviving cells relative to control populations. The results are expressed as the median cytotoxic concentrations (IC_{50} values) and were calculated from six-point dose response curves using fourfold serial dilutions.

Statistics: Data are expressed as mean ±SE for three replications on each cell line.

Supporting Information (see footnote on the first page of this article): Mass spectra, FTIR spectra, ^{1}H and ^{13}C NMR spectra, UV/Vis and fluorescence spectra.

Acknowledgments

This work was supported in part by the Mississippi INBRE funded by the National Centre for Research Resources/NIH (P20RR016476). The project was also supported in part by an award to F. A. B. from the National Institutes of Health (NIH) (Award Number P20RR16460). The authors acknowledge the National Science Foundation (NSF) for funding our ESI and MALDI-ToF mass spectrometers (grant number CHE 0639208). We are also grateful for our EMX^{micro} ESR spectrometer, which was funded by the NSF CRIF:MU Award # 0741991 and our new 400 MHz NMR spectrometer, which was funded by the NSF CRIF:MU Award # 0840390. A. A. H. is grateful for a USM Lucas Endowment Grant and funding from ExxonMobil Research and Engineering Company through Dr. John Robbins. We would like to thank Dr. Vijayaraghavan Rangachari and his research group for the use of their Cary Eclipse fluorescence spectrophotometer and Professor Glen Shearer for his constant positive motivation, which helped to mobilise this project. We thank Dr. Andrew Ozarowski of the National High Magnetic Field Laboratory (NHMFL, Tallahassee, FL, USA) for providing the ESR simulation programme used in this study.

[1] E. Wong, C. M. Giandomenico, *Chem. Rev.* **1999**, *99*, 2451–2466.
[2] a) M. Galanski, V. B. Arion, M. A. Jakupec, B. K. Keppler, *Curr. Pharm. Des.* **2003**, *9*, 2078–2089; b) M. A. Jakupec, M. Galanski, B. K. Keppler, *Rev. Physiol. Biochem. Pharmacol.* **2003**, *146*, 1–54.
[3] I. Ott, R. Gust, *Archiv der Pharmazie – Chemistry in Life Sciences* **2007**, *340*, 117–126.
[4] a) M. J. Clarke, *Coord. Chem. Rev.* **2003**, *203*, 209–233; b) M. J. Clarke, F. Zhu, D. R. Frasca, *Chem. Rev.* **1999**, *99*, 2511–2533; c) B. Armitage, *Chem. Rev.* **1998**, *98*, 1171–1200.
[5] D. d. O. Silva, *Anti-Cancer Agents Med. Chem.* **2010**, *10*, 312–323.
[6] F. A. Beckford, M. Shaloski Jr, G. Leblanc, J. Thessing, L. C. Lewis-Alleyne, A. A. Holder, L. Li, N. P. Seeram, *Dalton Trans.* **2009**, 10757–10764.
[7] a) P. Tarasconi, S. Capacchi, G. Pelosi, M. Cornia, R. Albertini, A. Bonati, P. P. Dall'Aglio, P. Lunghi, S. Pinelli, *Bioorg. Med. Chem.* **2000**, *8*, 157–162; b) D. X. West, J. K. Swearingen, J. Valdes-Martinez, S. Hernandez-Ortega, A. K. El-Sawaf, F. Van Meurs, A. Castineiras, I. Garcia, E. Bermejo, *Polyhedron* **1999**, *18*, 2919–2929.
[8] P. Noblia, M. Vieites, B. S. Parajon-Costa, E. J. Baran, H. Cerecetto, P. Draper, M. Gonzalez, O. E. Piro, E. E. Castellano, A. Azqueta, A. Lopez de Cerain, A. Monge-Vega, D. Gambino, *J. Inorg. Biochem.* **2005**, *99*, 443–451.
[9] a) O. J. D'Cruz, Y. Dong, F. M. Uckun, *Anti-Cancer Drugs* **2000**, *11*, 849–858; b) R. K. Narla, Y. Dong, P. Ghosh, K. Thoen, F. M. Uckun, *Drugs Future* **2000**, *25*, 1053–1068; c) O. J. D'Cruz, F. M. Uckun, *Expert Opin. Invest. Drugs* **2002**, *11*, 1829–1836; d) I. Fichtner, J. Claffey, A. Deally, B. Gleeson, M. Hogan, M. R. Markelova, H. Mueller-Bunz, H. Weber, M. Tacke, *J. Organomet. Chem.* **2010**, *695*, 1175–1181; e) D. Rehder, in: *Bioinorganic Vanadium Chemistry*, John Wiley & Sons, Chichester, UK, **2008**, p. 176.
[10] L. L. Koh, J. Ranford, W. Robinson, J. O. Svensson, A. L. C. Tan, D. Wu, *Inorg. Chem.* **1996**, *35*, 6466–6472.
[11] J. C. Pessoa, M. T. Duarte, R. D. Gillard, C. Madeira, P. M. Matias, I. Tomaza, *J. Chem. Soc., Dalton Trans.* **1998**, 4015–4020.
[12] I. Cavaco, J. C. Pessoa, M. T. Duarte, R. T. Henriques, P. M. Matias, R. D. Gillard, *J. Chem. Soc., Dalton Trans.* **1996**, 1989–1996.
[13] E. Viñuelas-Zahínos, F. Luna-Giles, P. Torres-García, M. C. Fernández-Calderón, *Eur. J. Med. Chem.* **2011**, *46*, 150–159.
[14] R. Venkatraman, H. Ameera, L. Sitole, E. Ellis, F. R. Fronczek, E. J. Valente, *J. Chem. Crystallogr.* **2009**, *39*, 711–718.
[15] T. S. Lobana, R. Sharma, G. Bawa, S. Khanna, *Coord. Chem. Rev.* **2009**, *253*, 977–1055.
[16] a) M. M. Mostafa, A. El-Hammid, M. Shallaby, A. A. El-Asmay, *Trans. Met. Chem.* **1981**, *6*, 303; b) D. X. West, A. E. Liberta, S. B. Padhye, R. C. Chikate, P. B. Sonawane, A. S. Kumbher, R. G. Yerande, *Coord. Chem. Rev.* **1993**, *123*, 49.
[17] H. Beraldo, W. F. Nacif, L. R. Teixeira, J. S. Reboucas, *Trans. Met. Chem.* **2002**, *27*, 85–88.
[18] a) T. B. Demirci, Y. Koseoglu, S. Guner, B. Ulkuseven, *Cent. Eur. J. Chem.* **2006**, *4*, 149–159; b) H. Zhang, R. Thomas, D. Oupicky, F. Peng, *J. Biol. Inorg. Chem.* **2008**, *13*, 47–55.
[19] a) I. C. Mendes, L. M. Botion, A. V. M. Ferreira, E. E. Castellano, H. Beraldo, *Inorg. Chim. Acta* **2009**, *362*, 414; b) J. C. Pessoa, I. Cavaco, I. Correia, I. Tomaz, T. Duarte, P. M. Matias, *J. Inorg. Biochem.* **2000**, *80*, 35–39.
[20] M. M. M. Raposo, B. Garcia-Acosta, T. Abalos, P. Calero, R. Martinez-Manez, J. V. Ros-Lis, J. Soto, *J. Org. Chem.* **2010**, *75*, 2922–2933.

[21] Z. Afrasiabi, E. Sinn, P. P. Kulkarni, V. Ambike, S. Padhye, D. Deobagakar, M. Heron, C. Gabbutt, C. E. Anson, A. K. Powell, *Inorg. Chim. Acta* **2005**, *358*, 2023–2030.
[22] V. Mahalingam, N. Chitrapriya, F. R. Fronczek, K. Natarajan, *Polyhedron* **2008**, *27*, 2743–2750.
[23] B. Baruah, S. Das, A. Chakravorty, *Inorg. Chem.* **2002**, *41*, 4502–4508.
[24] M. R. Maurya, S. Khurana, D. Rehder, *Trans. Met. Chem.* **2003**, *28*, 511–517.
[25] K. Nakajima, M. Kojima, K. Toriumi, K. Saito, J. Fujita, *Bull. Chem. Soc. Jpn.* **1989**, *62*, 760–767.
[26] N. Kanoongo, R. Singh, J. P. Tandon, *Trans. Met. Chem.* **1987**, *12*, 271–273.
[27] a) P. K. Sasmal, A. K. Patra, M. Nethaji, A. R. Chakravarty, *Inorg. Chem.* **2007**, *46*, 11112–11121; b) K. Toshima, R. Takano, T. Ozawa, S. Matsumura, *Chem. Commun.* **2002**, 212–213.
[28] a) S. P. Rath, T. Ghosh, S. Mondal, *Polyhedron* **1997**, *16*, 4179–4186; b) J. A. Bonadies, C. J. Carrano, *J. Am. Chem. Soc.* **1986**, *108*, 4088–4095.
[29] A. Ozarowski, H. M. Lee, A. L. Balch, *J. Am. Chem. Soc.* **2003**, *125*, 12606–12614.
[30] a) M. Branca, G. Micera, A. Dessi, D. Sanna, K. N. Raymond, *Inorg. Chem.* **1990**, *29*, 1586–1589; b) N. D. Chasteen, E. M. Lord, H. J. Thompson, J. K. Grady, *Biochim. Biophys. Acta Gen. Subj.* **1986**, *884*, 84–92; c) D. C. Crans, A. R. Khan, M. Mahroof-Tahir, S. Mondal, S. M. Miller, A. la Cour, O. P. Anderson, T. Jakusch, T. Kiss, *J. Chem. Soc., Dalton Trans.* **2001**, 3337–3345; d) K. Efthimiadou Eleni, G. Psomas, Y. Sanakis, N. Katsaros, A. Karaliota, *J. Inorg. Biochem.* **2007**, *101*, 525–535; e) S. K. Ghosh, R. Patra, S. P. Rath, *Inorg. Chem.* **2008**, *47*, 9848–9856; f) M. Mahroof-Tahir, A. D. Keramidas, R. B. Goldfarb, O. P. Anderson, M. M. Miller, D. C. Crans, *Inorg. Chem.* **1997**, *36*, 1657–1668; g) T. K. Paine, T. Weyhermueller, L. D. Slep, F. Neese, E. Bill, E. Bothe, K. Wieghardt, P. Chaudhuri, *Inorg. Chem.* **2004**, *43*, 7324–7338; h) Y. Z. Xu, S. Shi, *Appl. Magn. Reson.* **1996**, *11*, 1–6.
[31] a) G. Micera, E. Garribba, *J. Comput. Chem.* **2011**, *32*, 2822–2835; b) G. Micera, V. L. Pecoraro, E. Garribba, *Inorg. Chem.* **2009**, *48*, 5790–5796; c) G. Micera, E. Garribba, *Dalton Trans.* **2009**, 1914–1918; d) E. Garribba, E. Lodyga-Chruscinska, G. Micera, A. Panzanelli, D. Sanna, *Eur. J. Inorg. Chem.* **2005**, 1369–1382.
[32] W. L. Kan, C. H. Cho, J. A. Rudd, G. Lin, *J. Ethnopharmacol.* **2008**, *120*, 36–43.
[33] C. A. Puckett, R. J. Ernst, J. K. Barton, *Dalton Trans.* **2010**, *39*, 1159–1170.
[34] D. C. Crans, A. A. Holder, T. K. Saha, G. K. Prakash, M. Yousufuddin, R. Kultyshev, R. Ismail, M. F. Goodman, J. Borden, F. Florián, *Inorg. Chem.* **2007**, *46*, 6723–6732.
[35] G. M. Sheldrick, *Acta Crystallogr., Sect. A: Foundations of Crystallography* **2008**, *64*, 112–122.
[36] a) G. M. Sheldrick, *NATO ASI Series, Series E: Applied Sciences* **1997**, *347*, 219–230; b) G. M. Sheldrick, T. R. Schneider, *Methods Enzymol.* **1997**, *277*, 319–343.
[37] J. Vanco, O. Svajlenova, J. Marek, *Acta Crystallogr., Sect. C: Cryst. Struct. Commun.* **2003**, *59*, m190–m192.
[38] A. H. Cory, T. C. Owen, J. A. Barltrop, J. G. Cory, *Cancer Commun.* **1991**, *3*, 207–212.

Received: August 25, 2011
Published Online: December 28, 2011

